ELSEVIER

Chemical Engineering Journal 72 (1999) 53–61

Chemical Engineering Journal

Reaction kinetics and heat transfer studies in thermoset resins

A. Nzihou[a], P. Sharrock[b], A. Ricard[a,*]

[a]*Laboratoire de Génie Chimique CNRS UMR 5503-ENSIGC, 18 chemin de la Loge 31078, Toulouse Cedex, France*
[b]*Laboratoire de Chimie Inorganique, Université Paul Sabatier, IUT Chimie Castres 31062, Toulouse, France*

Received 5 January 1998; received in revised form 28 September 1998; accepted 6 October 1998

Abstract

The differential scanning calorimetry technique is used to study the polymerization kinetics of thermoset resins (bone cement), both under isothermal and dynamic conditions. A phenomenological kinetic model, which takes into account the diffusion effect, is proposed. The model, coupled with an energy balance, is used to predict the fractional conversion, the conversion rate and the temperature profile for different thicknesses of the resin. In isothermal conditions, the conversion is less than 1, giving proof of the presence of unreacted monomer in the resin. The results obtained under dynamic conditions indicate that the resulting temperature increase is responsible for the higher conversion and a better cure of the resin. Bone cement is intended for use in filling the gap between bone and metal prosthesis. For such cases, we have also noted that the prosthesis absorbs much heat and effectively cools the resin, whereas bone does not support a strong temperature elevation and is only locally in contact with hot cement at the bone–cement interface, and for a short time period. In this respect, the proposition of a workable model for cement polymerization may help in determining proper limits for cementation techniques.

Keywords: Kinetics; Heat transfer; DSC; Resin; Polymerization

1. Introduction

Acrylic resins, also called bone cement, are used for the fixation of joint prostheses to bone and for the repairing or prevention of bone fractures [1–5]. The pharmaceutical originality of bone cements lies in their use as drug carriers and as chirurgical material.

The production of bone cements consists of three steps: mixing of the solid and liquid phases (concentrated suspensions are obtained), gel formation and polymerization of the monomer. The solid phase includes poly(methylmethacrylate) beads, benzoyl peroxide (initiator), and radio-opaque substances like zinc oxide, zirconium dioxide and barium sulphate. The liquid phase contains the monomers: methylmethacrylate (MMA) and butylmethacrylate (BMA), and the accelerator, *N*,*N*-dimethylparatoluidine (*N*,*N*-DMPT). When the two phases are mixed and placed in situ with a syringe during the implantation of arthroprostheses, *N*,*N*-DMPT provokes the decomposition of benzoyl peroxide into free radicals, which initiate the polymerization reaction and the formation of entangled polymer chains.

The major problem involved with the cement is the heat generated during the polymerization [1–6]. The high local temperatures, reached due to the exothermic chain propagation reaction, have a deleterious effect on living cells and extracellular matrices. Such denaturation reactions lead to necrosis of adjacent tissues. In spite of such disadvantages, acrylic bone cements are still used because of their good mechanical properties and convenient handling characteristics.

The polymerization of thermoset resins implies the transformation of the suspension into a glassy solid (vitrification) as a result of a chemical reaction. Vitrification may strongly affect polymerization kinetics, causing the reaction to stop. In these conditions, the reaction becomes diffusion-controlled and the termination step is governed by the reduction in molecular mobility.

In this paper, isothermal and dynamic cure for the resin are described. In the first part, the reaction kinetics are analyzed by differential scanning calorimetry (DSC). DSC data are used for the quantitative determination of fractional conversion and conversion rate during the polymerization in isothermal and dynamic conditions. A kinetic model derived for thermosetting systems is presented.

*Corresponding author.

1385-8947/99/$ – see front matter
PII: S1385-8947(98)00137-5

This kinetic model is coupled with an energy balance in order to predict the temperature profile across the prosthesis, bone and resin, and the monomer conversion during the dynamic polymerization.

Temperature and fractional conversion reaction profiles are calculated as a function of setting time, taking into account the heat rate generated by the polymerization reaction, the system's geometry, the thermal conductivity of bone and prosthesis, and the variation of the thermal conductivity of the resin. Contrary to the results published in the literature [5–7], the variation of the heat capacity with the temperature and the conversion are considered and were introduced in the heat transfer equations.

Kinetic and heat transfer models were coupled and the system was solved by implementing a numerical method. The effects of the resin thickness and the initial cure temperature on the temperature and the extent of reaction profiles across the resin were investigated. The proposed model and the results obtained may, thus, help in determining the limits for cementation techniques.

2. Materials and methods

Samples used in this study were obtained by mixing solid and liquid components of commercial SULFIX-6. The liquid phase is composed of the monomers, methylmethacrylate (16.08 g), butylmethacrylate (2.84 g) and *N*,*N*-dimethyl paratoluidine (0.38 g). This phase is stabilized with hydroquinone monomethylether (0.544 mg).

The solid phase contains 42.38 g of poly(methylmethacrylate) powder characterized by a mean size $d_p = 60\ \mu m$ and an average molecular weight $M = 360\,000$ g/mole, benzoyl peroxide powder (0.8 g) with a mean size $d_p < 1\ \mu m$, hydroquinone and 4.76 g of inorganic radiopaque component (Zirconium dioxide, $d_p < 1\ \mu m$).

DSC was used for the study. The DSC analysis was carried out with a SETARAM DSC 92 operating with a constant nitrogen flow of 100 cm^3/min in the temperature range between 0°C and 250°C. The measurements were performed at 5°C/min, in both isothermal and non-isothermal mode on 8–11 mg samples. DSC measurements were carried out three times for each sample and data obtained were identical provided the same amount of components was weighed for each run.

In order to measure the temperature rise inside the cement, the suspension containing the polymer, the monomer and zirconium dioxide was introduced in a teflon insulated cylindrical reactor of 7 cm^3 (Fig. 1). The temperature was given by a thermocouple. The reproducibility of the measured temperatures inside the cement was checked for three runs.

3. Polymerization kinetics

A typical thermogramme obtained with a reacting mixture described in Section 2 at 25°C is reported in Fig. 2,

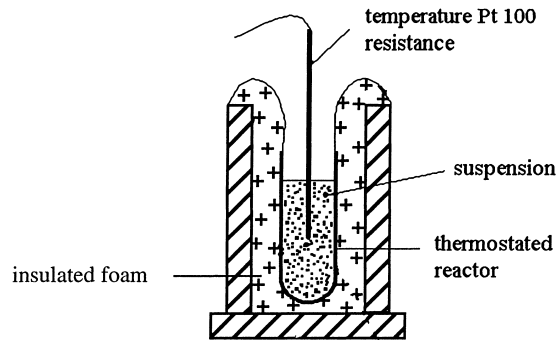

Fig. 1. Schematic experimental setup.

where the delay in the DSC signal represents the induction time t_i, which is associated with the reaction between the initiator and the inhibitor [8,9].

The induction time t_i may be considered as the only detectable macroscopic parameter representative of the inhibitor–initiator reaction. It shows the following temperature dependence:

$$t_i = \frac{1}{K_0 \times \exp(-E_a/RT)} \quad (1)$$

The induction times, determined in different isothermal DSC experiments are represented in Fig. 3. The activation energy E_a and the pre-exponential constant K_0 were calculated and are reported in Table 1. These values are comparable to data found in the literature for similar materials [5–7,10,11].

DSC measurements may be used for determining the progress of curing by assuming that the heat evolved during the polymerization reaction is proportional to the overall extent of reaction given by the relative fraction of reagents consumed. Following this approach, the degree of reaction, α, is defined as

$$\alpha = \frac{Q_{is}(t)}{Q_{tot}} \quad (2)$$

where $Q_{is}(t)$ (kJ/g) is the partial heat of reaction released at time t during an experiment carried out in isothermal

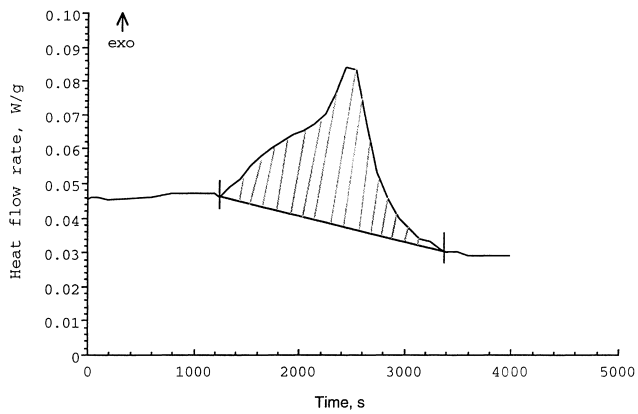

Fig. 2. Isothermal DSC thermogramme obtained during polymerization. $T = 25$°C, volume concentration of solids $\phi = 0.4$.

Table 1
Parameters obtained from calorimetric measurements

a (kJ/g)	b (kJ/g)	c	d (K^{-1})	K_0 (s^{-1})	E_a (kJ/mol)	Q_{tot} (kJ/g)
0.004	0.002	−4.666	0.0168	4.76×10^9	71.41	0.152

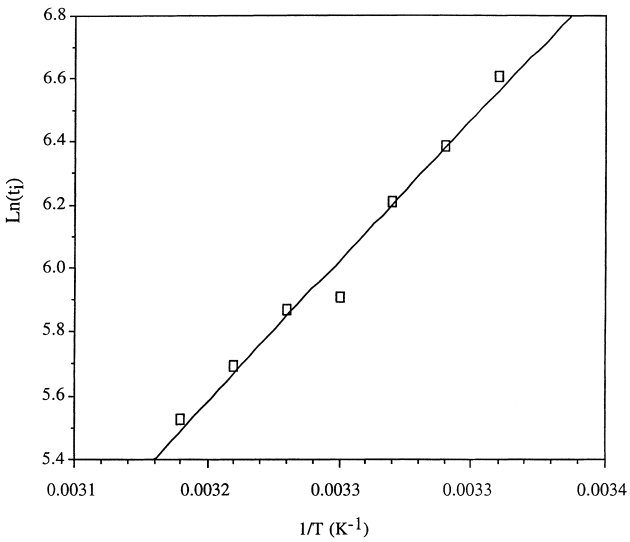

Fig. 3. Isothermal induction time vs. temperature.

conditions and Q_{tot} (kJ/g) represents the maximum heat of reaction measured by DSC. The reaction rate, $d\alpha/dt$, is given by

$$\frac{d\alpha}{dt} = \frac{1}{Q_{tot}} \left(\frac{dQ}{dt}\right)_{is} \quad (3)$$

The isothermal heat of reaction $Q_{is}(t)$ (for $t = 20$ min) shows a linear dependence on the cure temperature as given in Eq. (4), and illustrated in Fig. 4.

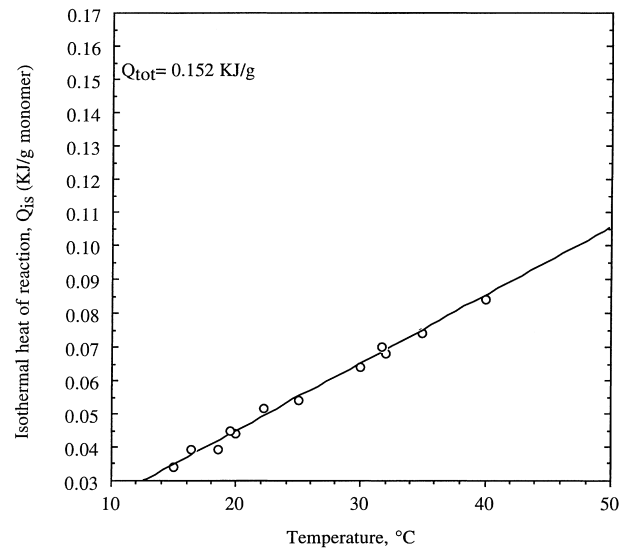

Fig. 4. Temperature dependence of the isothermal heat of reaction at $\phi = 0.4$.

$$Q_{is}(t) = a + bT \quad (4)$$

where T is expressed in °C.

A good agreement between predictions by this equation and experimental data is observed using the parameters listed in Table 1.

Q_{tot} has been determined from scanning experiments (20–180°C) and found to be equal to 0.152 kJ/g.

The heat released during isothermal experiments is lower than Q_{tot} found for a total conversion, indicating that unreacted monomer is still present. Therefore, at any temperature, the maximum degree of reaction, α_m, is expressed by

$$\alpha_m = \frac{Q_{is}}{Q_{tot}} \quad (5)$$

The temperature dependence of the maximum conversion of monomers, α_m, shown in Fig. 5 is linear as has also been observed for other systems [6,12,13]

$$\alpha = c + dT \quad (6)$$

where T is expressed in K. Parameters c and d are reported in Table 1.

3.1. Kinetic modelling

The most common kinetic model with an empirical nth order reaction is represented by the following equation:

$$\frac{d\alpha}{dt} = K(1-\alpha)^n \quad (7)$$

where n is the reaction order, α the degree of reaction and K is the temperature-dependent kinetic constant defined by

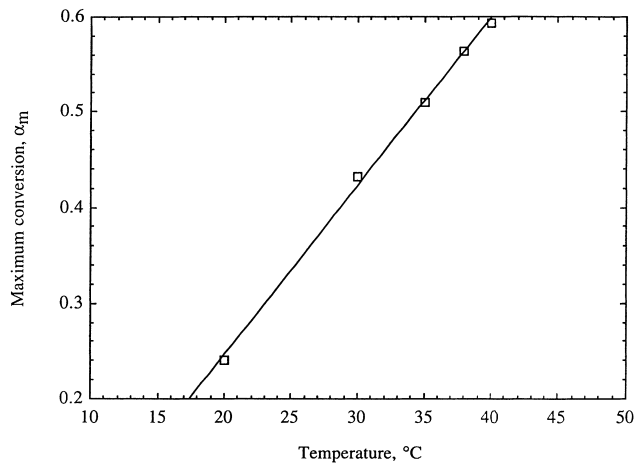

Fig. 5. Variation of monomer conversion with temperature.

Eq. (8)

$$K = K_0 \exp\left(\frac{E_a}{RT}\right) \tag{8}$$

where K_0 (s^{-1}) is the pre-exponential factor, E_a (kJ/mol) the activation energy (see Table 1), R (kJ/mol K) the gas constant and T (K) the absolute temperature.

For radical polymerization initiated by thermal decomposition of an initiator, the kinetic equation is given by

$$\frac{d\alpha}{dt} = k_{pr}\left(\frac{2fk_iI}{k_t}\right)^{0.5} \times (1-\alpha) \tag{9}$$

where k_{pr}, k_i, and k_t represent the kinetic constants of propagation, initiation and termination reactions, f the initiator efficiency and I the initiator concentration.

This equation is valid only for constant temperatures in steady state conditions [14] and low monomer conversions ($\alpha < 0.20$). However, polymerization reactions are characterized by the effect of the diffusion of the reagents occurring for high conversions that is due to the increase in viscosity of the reacting mixture (gel and glass effects). These effects are particularly important for MMA polymerization. Many complex models have been reported in the literature for the polymerization of MMA [15]. Since the gel and glass effects cause a decrease of k_t and k_{pr} as the reaction is in progress, these kinetic constants may be considered dependent on the degree of reaction as follows:

$$k_t = k_t' \alpha^{-2l} \tag{10}$$

$$k_{pr} = k_{pr}'(\alpha_m - \alpha)^n \tag{11}$$

where α_m is the maximum monomer conversion at a given temperature T. Therefore, taking into account the change of k_{pr} and k_t with conversion Eqs. (10) and (11), the polymerization rate equation is the following:

$$\frac{d\alpha}{dt} = K \times \alpha^A(\alpha_m - \alpha)^B \times (1-\alpha) \tag{12}$$

Eq. (12) was solved using a classical Runge–Kutta Merson numerical method. The required initial conditions are the degree of reaction at time zero, and the temperature range. The parameters of Eq. (12) have been identified by fitting the model with experimental data, so the equation becomes:

$$\frac{d\alpha}{dt} = 4.76 \times 10^9 \exp\left(\frac{-8582}{T}\right) \times \alpha^{1.7}(0.0168\,T - 4.666 - \alpha)^{0.9} \times (1-\alpha) \tag{13}$$

The experimental DSC data obtained in isothermal conditions and the model predictions reported in Figs. 6 and 7 are in good agreement.

From the experimental kinetic curves (Fig. 6) obtained at 20°C, 25°C, 30°C and 40°C, the maximum rates of conversion have been found equal to 0.24, 0.39, 0.43 and 0.6 respectively. These values, lower than 1, give the proof of the presence of unreacted monomer in the cement. Indeed, residual monomer can cause, in part, the toxicity of the bone cement.

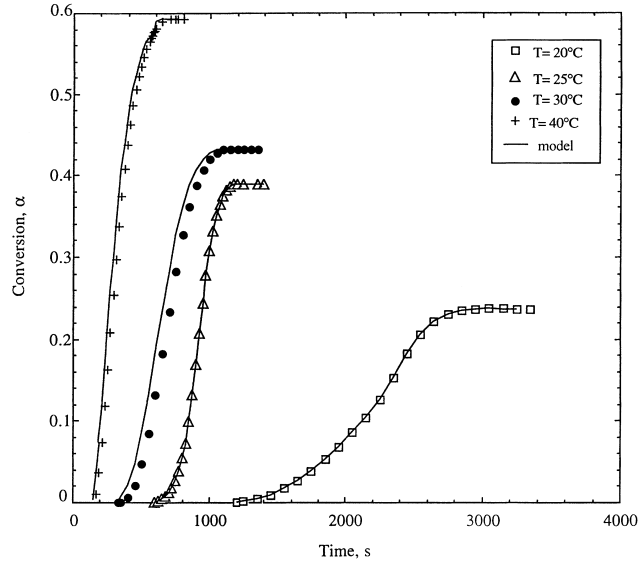

Fig. 6. Conversion vs. time: comparison between kinetic model predictions and experimental data at several temperatures in isothermal conditions.

The unreacted monomer can be polymerized by heating the cement at temperature up to 130°C as shown in Fig. 8.

The DSC analysis of the cement allows the calculation of the degree of conversion during curing, and the conversion rate at different temperatures using the heat flow of the polymerization reaction. Also, the kinetic study has shown the presence of unreacted monomer by heating the sample further after an isothermal polymerization experiment.

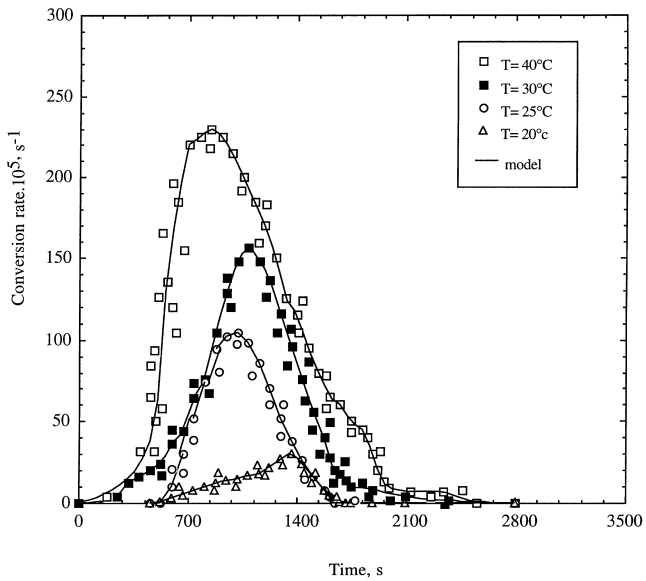

Fig. 7. Reaction rate vs. time: comparison between kinetic model predictions and experimental data at several temperatures in isothermal conditions.

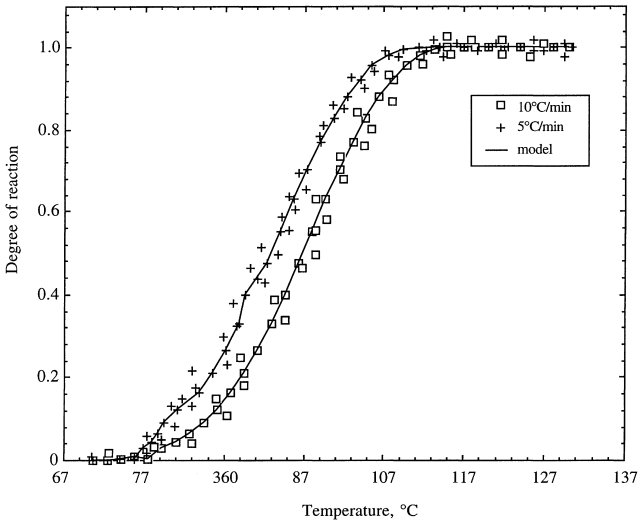

Fig. 8. Comparison between kinetic model predictions and experimental data conversion vs. time: non-isothermal conditions.

Finally, experimental data and model predictions in isothermal conditions show a good agreement (Figs. 6–8). Thus, the model Eq. (13) can be used to predict the curing kinetics of bone cement, and it has been introduced in the relation established to stimulate the heat transfer in the cement and around it (bone and prosthesis) as shall be presented in the next section.

4. Heat transfer

4.1. Simulation

The exothermic nature of the polymerization reaction induces heat generation in the material during curing. For a thick layer, all the heat cannot be dissipated fast enough to maintain isothermal conditions. The material properties and the polymerization conditions determine whether the highest temperature is in the core, at the skin or at an intermediate position in the composite thickness. Fig. 9 shows the geometry of the composite and its environment which was considered for calculation. The temperature profile within the material can be calculated by solving an energy balance coupled with an appropriate expression for the cure kinetics [5–7,16,17]. The energy balance equations (cylindrical geometry) for the bone, cement and prosthesis coupled with the kinetic expression are given by:

$$\rho_p \times Cp_p \times \frac{\partial T}{\partial t} = \lambda_p \times \frac{1}{R'} \times \frac{\partial T}{\partial R'} + \lambda_p \times \frac{\partial^2 T}{\partial R'2} \quad 0 < R' < R'_p \tag{14}$$

$$\rho_c \times Cp_c \times \frac{\partial T}{\partial t} = \lambda_c \times \frac{1}{R'} \times \frac{\partial T}{\partial R'} + \lambda_c \times \frac{\partial^2 T}{\partial R'2} + \rho_c \frac{dQ}{dt} \quad R'_p < R' < R'_c \tag{15}$$

$$\rho_b \times Cp_b \times \frac{\partial T}{\partial t} = \lambda_b \times \frac{1}{R'} \times \frac{\partial T}{\partial R'} + \lambda_b \times \frac{\partial^2 T}{\partial R'2} \quad R'_c < R' < R'_b \tag{16}$$

where dQ/dt is the rate of heat generation due to the reaction in the cement and defined as follows:

$$\frac{dQ}{dt} = Q_{tot}\left(\frac{d\alpha}{dt}\right) \tag{17}$$

$d\alpha/dt$ is the reaction rate given by Eq. (12).

These equations are valid for the following assumptions:

1. Heat is dissipated only in the radial direction (R' axis).
2. Mean densities and thermal conductivities of bone and core are used and no variation of these properties as a function of the temperature and/or degree of reaction is considered. These values are reported in Table 2.

4.1.1. Determination of the heat capacity of the cement

Bailleul et al. [18] have shown the dependence of the heat capacity of the composite Cp_c with the temperature and the conversion in non-isothermal conditions. In their approach, the fraction of cured sample, α, is taken into account (from $\alpha = 0$ to $\alpha = 1$). Thus, they define the heat capacity of the composite as

$$Cp_c = Cp(\alpha, T) = Cp_1(T) \times \alpha + Cp_0(T) \times (1 - \alpha) \tag{18}$$

where $Cp_0(T)$ is the temperature dependent heat capacity per unit of mass of the unreacted fluid mixture and $Cp_1(T)$, the

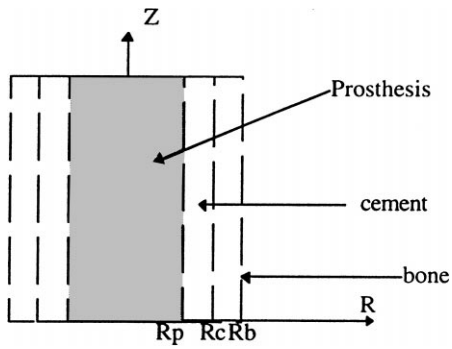

Fig. 9. Sketch of the geometry of the system used for the simulation of heat transfer

Table 2
Parameters for Eqs. (14) and (15) and Eq. (16)

Parameter	Prosthesis	Cement	Bone
λ (W/m K)	10.3	0.17	0.43
Cp (kJ/g K)	500	Cp_c^*	1250
ρ(kg/m^3)	7800	1100	1700

* The determination of the heat capacity (Cp_c) of the cement is discussed in Section 4.1.1.

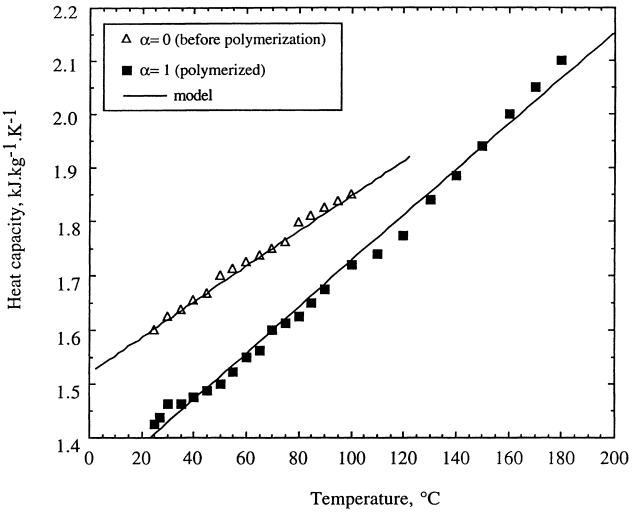

Fig. 10. Heat capacity as a function of temperature for $\alpha = 0$ and $\alpha = 1$.

heat capacity per unit of mass of the cement (transformed mixture).

$$\mathrm{Cp}_0(T) = A_0 + B_0 T \tag{19}$$

Schematically, the heat generated within the sample is composed of two terms [18], the first takes into account the conductive heat and the second, the exothermicity of the reaction:

$$Q(t) = -m\,C_\mathrm{p}\,\frac{\mathrm{d}T}{\mathrm{d}t} + m\,\Delta H\,\frac{\mathrm{d}\alpha}{\mathrm{d}t} \tag{20}$$

The last term is equal to zero for $\alpha = 0$ and $\alpha = 1$

As the reaction is irreversible, the heat capacity of the transformed material Cp_1 is easily determined by DSC and depends on temperature as:

$$\mathrm{Cp}_1(T) = A_1 + B_1 T \tag{21}$$

Results obtained for $\mathrm{Cp}_0(T)$ and $\mathrm{Cp}_1(T)$ are represented in Fig. 10.

Contrary to the results published in the literature [5–7], a significant variation of the heat capacity as a function of temperature and conversion is observed with the system examined. Data also show that the heat capacity of the unreacted mixture is higher than that of the composite. This trend was also observed by Bailleul et al. [18,19]. Therefore, the variation of C_p with temperature must be taken into account when solving the energy balance.

4.1.2. Solving of the heat transfer equation

Dimensionless numbers have been introduced to solve the set of thermal equations:

- $\theta = (T - T_0)/(T_\mathrm{ref} - T_0)$, where $T_0 = 20^\circ\mathrm{C}$ is the temperature of the cement at $t = 0$, and $T_\mathrm{ref} = 37^\circ\mathrm{C}$, the temperature of the bone.
- $r = R'/R'_0$.

The boundary conditions are:

- At $t = 0$, $T_\mathrm{(p,c)} = 20^\circ\mathrm{C}$ and $T_\mathrm{b} = 37^\circ\mathrm{C}$.
- For $r = 0$, $\partial T/\partial R' = 0$.

The kinetic equation given by Eq. (13) is introduced in the heat transfer equation and the energy balance is solved using a finite-difference method, according to the semi-implicit schema of Crank-Nicholson [20,21]:

$$\frac{\lambda}{2\Delta r}\left(\frac{\theta_{i+1}^{k+1} - \theta_i^{k+1}}{\Delta r} - \frac{\theta_i^{k+1} - \theta_{i-1}^{k+1}}{\Delta r}\right) + \frac{\lambda}{2\Delta r}\left(\frac{\theta_{i+1}^{k} - \theta_i^{k}}{\Delta r} - \frac{\theta_i^{k} - \theta_{i-1}^{k}}{\Delta r}\right) - \rho \mathrm{Cp}_i^{k+1/2}\,\frac{\theta_i^{k+1} - \theta_i^{k}}{\Delta t} = \rho (Q_\mathrm{tot})_i^{k+1/2}\left(\frac{\alpha_i^{k+1} - \alpha_i^{k}}{\Delta t}\right) \tag{22}$$

This numerical method takes into account the non-linearity of the kinetics and heat equations.

4.1.3. Simulation results and discussion

The results presented in this section were obtained with the composite containing zirconium dioxide as filler. The thickness of the different layers: prosthesis, cement and bone and the initial and boundary conditions are mentioned in the previous section.

As the cement has a poor conductivity, the effect of its thickness has been investigated. Figs. 11 and 12 give the results obtained from simulations, showing respectively, the temperature evolution and the degree of reaction as a function of the cure time at the bone–cement interface.

The effect of the temperature variation through the various layers is clearly shown. A very high rate of generated heat, coupled with the thermal conductivity causes a strong temperature increase in the cement. Because of a higher temperature in the part closer to the cement–bone interface, the rate of the cement curing is faster than in the cement which is in contact with the prosthesis (at $T = 20^\circ\mathrm{C}$) where

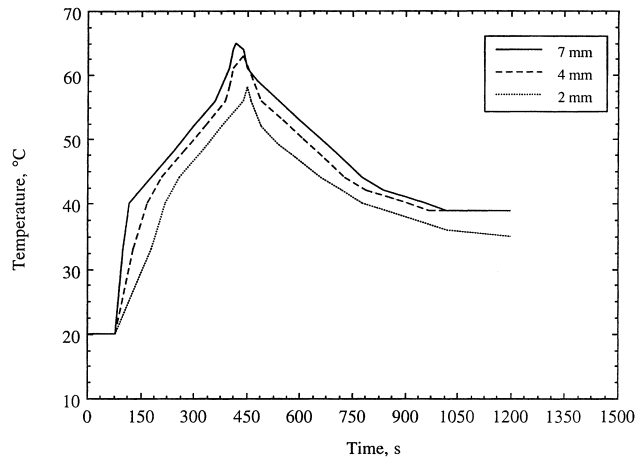

Fig. 11. Temperature vs. cure time at the bone–cement interface for different layer thicknesses. Initial boundary condition $T_0 = 20^\circ\mathrm{C}$.

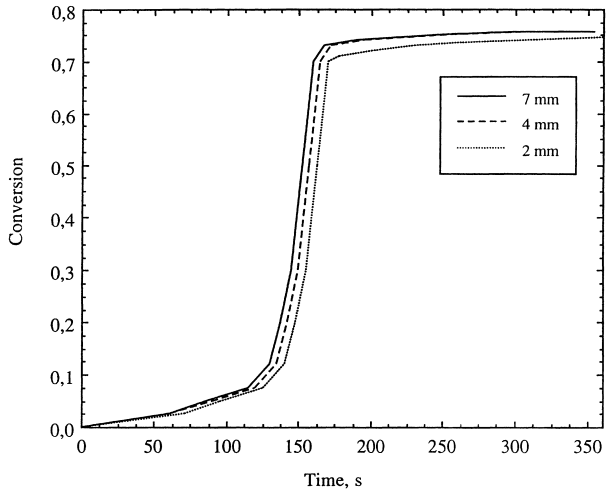

Fig. 12. Conversion vs. cure time at the bone–cement interface for different layer thicknesses. Initial boundary condition $T_0 = 20°C$.

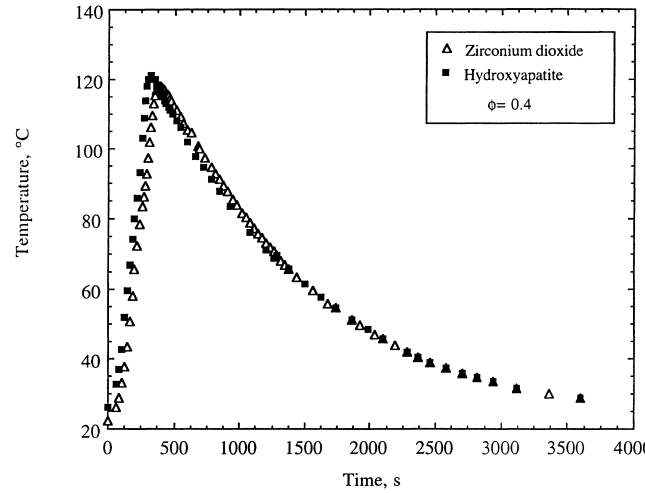

Fig. 14. Experimental temperature variation with time in the composite for different fillers and with a constant solid concentration.

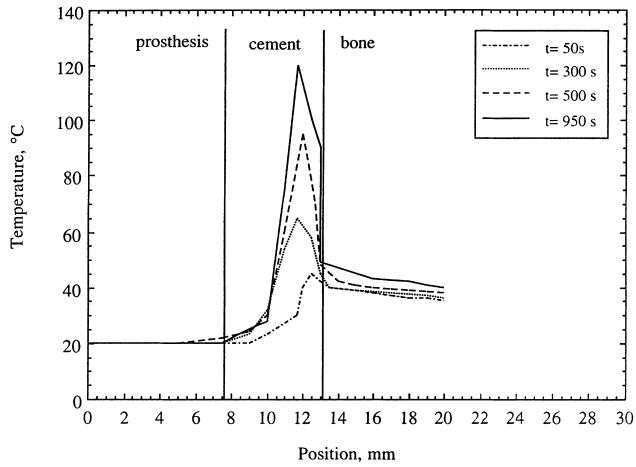

Fig. 13. Simulation of the temperature profiles across prosthesis, bone and cement at different time intervals.

the cure follows kinetics which is governed by isothermally imposed temperatures.

When the balance between heat generation and thermal conductivity is obtained, the temperature profile reaches a maximum. The highest temperature is reached on the skin of the restoration as a consequence of the poor heat dissipation at the interface with air in the cavity.

Fig. 11 also shows that the reaction starts simultaneously at every point across the cement thickness, determining a peak temperature at the bone–cement interface of about 60°C, while, in the core of the layer, the temperature is higher than 120°C (Fig. 13). The metal of the prosthesis acts as an effective heat sink and prevents temperature elevation in the cement at a distance of up to 2 mm from the prosthesis–cement interface. The temperature elevation inside the prosthesis remains negligible. It must be noted that the high temperature reached inside the cement leads to a final degree of reaction close to 1 (Fig. 8). For this reason, the average value of α for the whole cement at the end of the polymerization is, indeed, higher than that shown in Fig. 12.

Some authors [5–7] have pointed out that the temperature threshold for thermal tissue damage is in the range of 50°C to 60°C, depending on the exposure time. At 60°C, cell necrosis occurs with an exposure time between 30 and 400 s. However, if a too high temperature increase is detrimental for the tissues in contact with the cement, it has a positive effect by enabling to reach a higher rate of conversion.

Briefly, an increase of the cement thickness affects the exposure time at the highest temperature rather than the maximum value of the temperature at the bone–cement interface. According to the polymerization mechanism described in Section 3, minimizing the peak temperature and maximizing the degree of reaction are two objectives that cannot be achieved simultaneously.

4.2. Experimental results

The results presented in this section are obtained from experiments carried out in a cylindrical reactor (Fig. 1) containing PMMA powder, MMA and ZrO_2 or hydroxyapatite, initiator and *N*,*N*-DMPT. When polymerization occurs, the system is characterized by an important heat generation in the composite (Fig. 14).

The maximum temperature determined experimentally is around 120°C, as predicted by simulation. Nevertheless, the conditions used in experiments and in the model calculations are not comparable. In fact, the cyclindrical reactor is insulated and does not exchange heat with the exterior environment, contrary to the case of bone repair where the heat is transferred from the cement to the bone and the prosthesis. However, if we consider

only the temperature reached inside the cement, a good agreement between the model and experimental data is obtained.

5. Conclusions

The polymerization kinetics of a mixture to produce a commercial thermoset resin charged with inorganic particles was investigated by Differential Scanning Calorimetry in isothermal and dynamic conditions. This technique has allowed the determination of fractional monomer conversion and conversion rate during the polymerization for different temperatures.

A phenomenological kinetic model, which accounts for diffusion effects, is proposed for the curing reaction. The model, which predicts the monomer conversion with time, is in good agreement with experimental data.

Under isothermal conditions the conversion α is less than 1 due to the presence of unreacted monomer in the resin. However, the results obtained under dynamic conditions indicate that the temperature increase is responsible for higher conversion and better cure of the resin. Therefore, the high temperature reached by the resin is required to guarantee complete polymerization and good functional properties, despite the undesirable side effects such as thermal denaturation of proteins and osteonecrosis. In fact, in acrylic bone cementation technique, isothermal conditions are not achieved; the reaction is exothermic and the temperature rise in the composite will depend on time and space. Bone cement is generally used to fix a prosthesis in a bone. So, we have considered that three layers make up the system: the prosthesis, the cement and the bone and we have assumed a cylindrical geometry. After introducing the cement and the prosthesis in the bone, heat is generated, due to polymerization reaction, and heat transfer in the different layers has been modelled. The model has been established from the energy balance in the bone, the cement and the prosthesis which leads to a set of differential equations. These equations were coupled with the reaction kinetics and solved using a finite difference method according to a semi implicit schema of Crank–Nicholson. Simulation results give the temperature profiles across the bone cement and the prosthesis. The model can also predict the variation of temperature and monomer conversion with time at the bone cement interface for different cement layer thicknesses. So, we have noted that the prosthesis absorbs much heat and effectively cools the resin, whereas bone does not suffer a strong temperature rise and is only locally exposed to hot cement at the bone-cement interface, and for a short time period. Results obtained from the simulation are in agreement with experimental data.

The proposition of a workable model for cement polymerization may help in determining proper limits for cementation techniques.

6. Nomenclature

A_0, B_0	constants for Eq. (19)
A_1, B_1	constants for Eq. (21)
Cp_0	heat capacity per unit of mass of the cement (kJ/kg K)
Cp_1	heat capacity of the polymerized cement (kJ/kg K)
Cp_c	heat capacity of the cement (kJ/kg K)
Cp_b	heat capacity of bone (kJ/kg K)
Cp_p	heat capacity of the prosthesis (kJ/kg K)
E_a	activation energy (kJ/mol)
f	initiator efficiency
ΔH	molar enthalpy of the reaction (kJ/g)
I	initiator concentration (mole/l)
k_i	kinetic constant of initiation (s^{-1})
k_{pr}	kinetic constant of propagation (l/mol s)
k_t	kinetic constant of termination (l/mol s)
K_0	pre-exponential constant (s^{-1})
K	kinetic constant of the global reaction (s^{-1})
$Q(t)$	heat of reaction (kJ/g)
r	dimensionless radius
R	gas constant (kJ/mol K)R'_b radius of the bone layer
R'_{pr}	radius of the prosthesis layer
R'_c	radius of the cement layer$T$ temperature (K)
T_{ref}	reference temperature (K)
α	fractional conversion
λ_b	thermal conductivity of the bone (W/m K)
λ_c	thermal conductivity of the cement (W/m K)
λ_{pr}	thermal conductivity of prosthesis (W/m K)
ρ_b	density of the bone (kg/m^3)
ρ_c	density of the cement (kg/m^3)
ρ_{pr}	density of the prosthesis (kg/m^3)
θ	dimensionless temperature
t_i	isothermal induction time (s)

Subscript

b	bone
c	cement or resin
g	glass transition
i	initiation
is	isothermal
m	maximum
n	reaction order
p	prosthesis
pr	propagation
ref	reference
t	termination
tot	total

References

[1] J. Charnley, J. Wrightington, J. Bone Joint Surg. (Br) 47 (1965) 354.
[2] R.C. Turner, P.E. Atkins, M.A. Ackley, J.B. Park, J. Biomed. Mater. Res. 15 (1981) 425.
[3] J.B. Park, R.S. Lakes, Biomaterials. An introduction, 2nd ed., Plenum Press, New York, 1992, p. 154.
[4] M.P. Ginebra, F.X. Gil, J.A. Planell, B. Pascual, I. Goni, M. Gurruchaga, B. Levenfeld, B. Vasquez, J.S. Roman, J. Mater. Sci. Mater. Med. 7 (1996) 375.
[5] A. Maffezzoli, D. Ronca, D. Guida, I. Pochini, L. Nicolais, J. Mater. Sci. Mater. Med. 8 (1997) 75.
[6] A. Maffezzoli, R. Terzi, L. Nicolais, J. Mater. Sci. Mater. Med. 6 (1995) 155.
[7] A. Maffezzoli, A. Della Pietra, S. Rengo, L. Nicolais, G. Valletta, Biomaterials 15 (1994) 1221.
[8] W.W.M. Wendlandt, Thermal Methods of Analysis, 3rd ed., Wiley, New York, 1993.
[9] A. Turi, Thermal Characterization of Polymeric Materials, Academic Press, San Diego, USA, 1981, pp. 3–46.
[10] J.M. Yang, J.S. Shyu, H.L. Chen, Polym. Eng. Sci. 37 (1997) 1182.
[11] J.M. Kenny, A. Maffezzoli, A. Nicolais, Compos. Sci. Tech. 38 (1990) 339.
[12] J.M. Kenny, A. Maffezzoli, A. Nicolais, Polym. Eng. Sci. 38 (1990) 339.
[13] J.M. Kenny, A. Trivisano, Polym. Eng. Sci. 31 (1991) 1426.
[14] G. Odian, Principles of Polymerization, McGraw-Hill, New York, 1991.
[15] S.T. Balke, A.E. Hamielec, J. Appl. Polym. Sci. 17 (1973) 905.
[16] F. Kreith, Principles of Heat Transfer, Dun-Donnelley Publishers, New York, 1973.
[17] R.B. Bird, W.E. Stewart, E.N. Lightfoot, Transport Phenomena, Wiley, New York, 1960.
[18] J.L. Bailleul, G. Guyonvarch, B. Garnier, Y. Jarny, D. Delaunay, Rev. Gén. Therm. 35 (1996) 65.
[19] G. Guyonvarch, M. Recouvreur, B. Soufflet, B. Garniet, D. Delaunay, Colloque Société Française de Thermique, Nantes, March 1994.
[20] B. Carnahan, H.A. Luther, J.O. Wilkes, Applied Numerical Methods, Krieger, Malabar, FL, USA, 1990.
[21] M. Minoux, Programmation Mathématique, Théorie et Algorithmes, Tome 1 et 2, Dunod, 1983.